Quart. J. R. Met. Soc. (1980), **106**, pp. 313–325

551.515.81 : 551.555.6

A case study of a subsynoptic disturbance in a polar outbreak

By J. OERLEMANS

Royal Netherlands Meteorological Institute, De Bilt, The Netherlands

(Received 27 March 1979; revised 15 August 1979. Communicated by Dr A. P. M. Baede)

SUMMARY

A subsynoptic disturbance, occurring in an outbreak of polar air over northwestern Europe, is studied by using routine observational data. The disturbance showed a characteristic length scale of about 150 km, a time scale of 4 hours, caused a surface pressure drop of only 1 mb, but brought up to 20 mm of precipitation in the coastal region of the Netherlands.

The observational analysis suggests that the disturbance was a warm-core system driven by latent heat release and triggered by forced lifting along the coastline, which activated a weak trough filled with potentially unstable air.

1. INTRODUCTION

During the night of 17–18 Nov. 1977, radar echoes of precipitation detected at Schiphol Airport (near Amsterdam) showed a very interesting feature. Figure 1 displays it by means of a series of hourly precipitation patterns. At 23 GMT (which corresponds to 24 local time) the shower activity over the North Sea region northwest of the Dutch coast suddenly increased and during the next two hours low-level inflow seems to have been present over the Netherlands. After that, a vortex-like disturbance developed which disappeared rapidly after 06 GMT. At 07 GMT the pattern no longer showed an organized structure. The time scale of the disturbance was about 4 hours and its length scale appeared to be roughly 150 km, which puts it among the so-called subsynoptic eddies. As will be shown in a later section, the pressure drop associated with the disturbance was only 1 mb. Nevertheless, precipitation amounts were up to 20 mm in the coastal region.

Since the eddy occurred in an outbreak of polar air over a warm sea, at first sight one may associate it with the polar low phenomenon. However, the smaller time-scale and the fact that the eddy seems to have been fixed by the coastline make it distinct from polar lows, which are more or less free modes of the flow (e.g. Harrold and Browning 1969; Rasmussen 1979; Økland 1977).

In general, diagnostic studies of disturbances in an outbreak of polar air over warm water are difficult to carry out because of lack of observational data. Therefore, little is known about these disturbances. There is a clear need to understand them because they have a pronounced influence on the weather and may ruin short-range forecasts completely. The eddy shown in Fig. 1 provided a good opportunity for a case study. The data used are from routine observations only; they appeared to give very useful information.

In the following sections we will investigate the disturbance by means of a detailed pressure analysis, a short discussion of the boundary-layer structure, and an examination of the computed convergence and vorticity in the region of interest. Based on these observational aspects a physical interpretation will be given.

2. THE SYNOPTIC SITUATION

Figure 2 shows the surface analysis of 00 GMT. The circulation was determined by an anticyclone west of the British Isles and an extensive area of low pressure over eastern

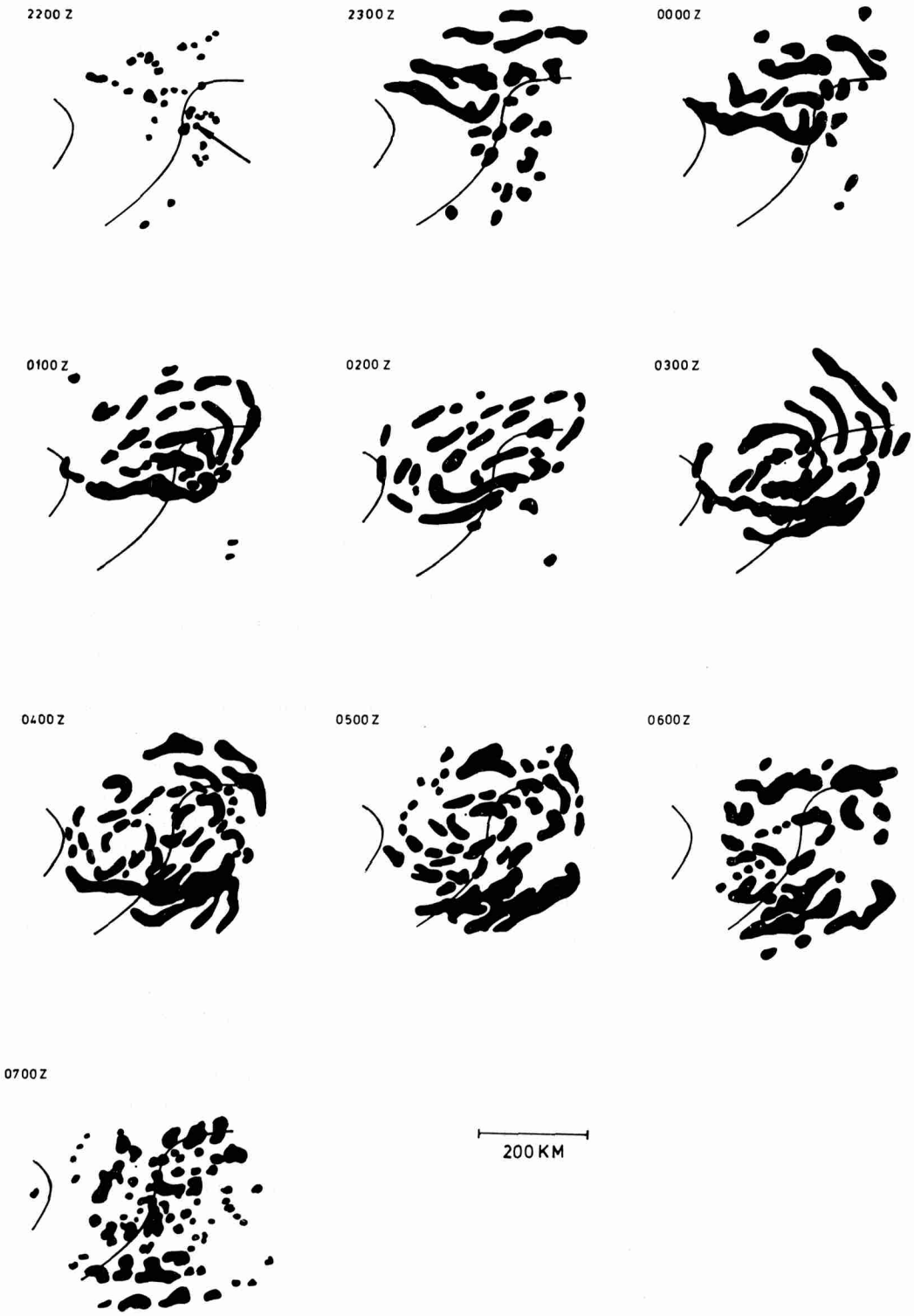

Figure 1. Hourly radar echoes of precipitation (sketches) detected at Schiphol Airport. The coastlines of the Benelux and East Anglia are indicated by thin lines. The arrow in the top-left picture shows the position of the radar. Tops ranged from 3 to 6·5 km.

Europe. Cold polar or even Arctic air flowed southwards over western Europe while it was heated from below in maritime regions. In this airflow, shower activity occurred frequently. In the vicinity of the southern North Sea region no frontal zones were present, but a weak trough, with the axis along the line Denmark–central England, approached the Benelux and northern Germany.

Figure 3 presents the analyses of the 850 and 500 mb level. At the 500 mb level a flow of a diffluent nature occurred over the North Sea. The 300 mb analysis (not shown here)

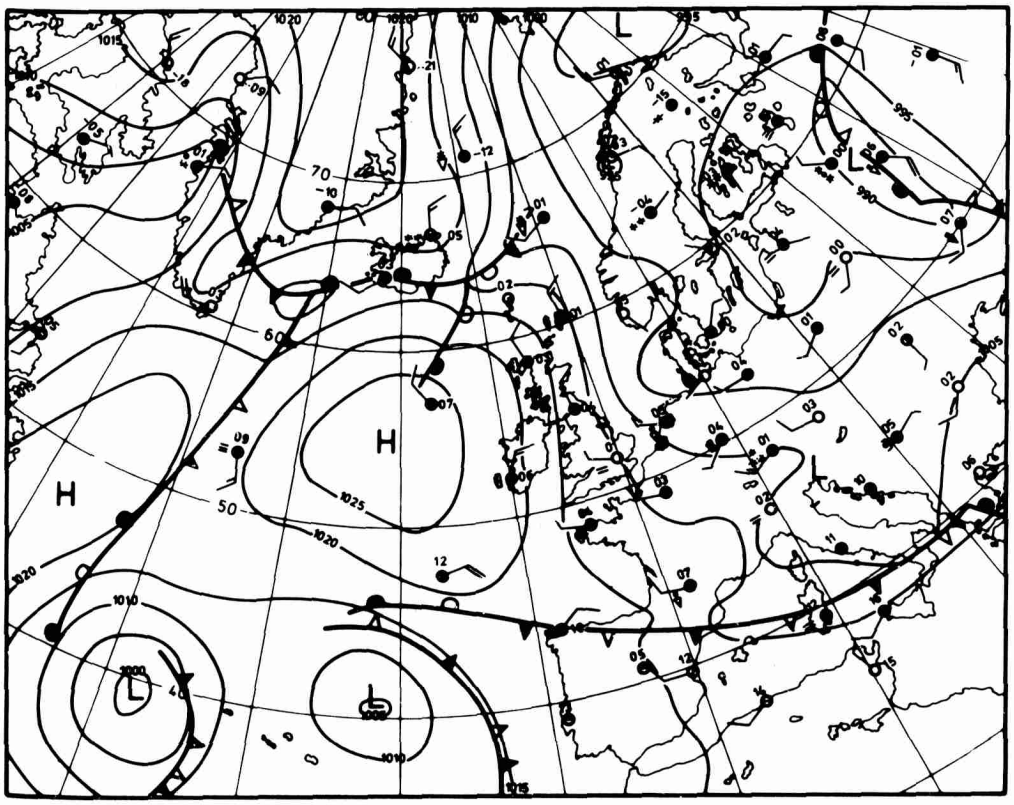

Figure 2. Surface analysis of 00 GMT, 18 November 1977.

revealed the presence of a jet stream running over Iceland–Ireland–southern France–Yugoslavia. Rawinsonde ascents of Hemsby (East Anglia), De Bilt (The Netherlands), Schleswig and Essen (Germany) and St Hubert (Belgium) all showed a conditionally unstable lapse rate while vertical wind shear was rather weak. The tropopause was situated around 330 mb.

During the evening, cloud cover decreased rapidly over the Netherlands and surface temperatures quickly dropped to 1–4°C. In contrast, sea surface temperatures in the southern North Sea were as high as 12°C. Consequently, a stable layer developed over land (with the inversion height varying between 20 and 200 m) while over the North Sea a highly unstable boundary layer prevailed day and night. The shower activity of the subsynoptic disturbance was considerable. Precipitation amounts up to 20 mm were reported by stations along the coast. In the most extensive precipitation zone (southern part of the eddy, see Fig. 1) thunder occurred.

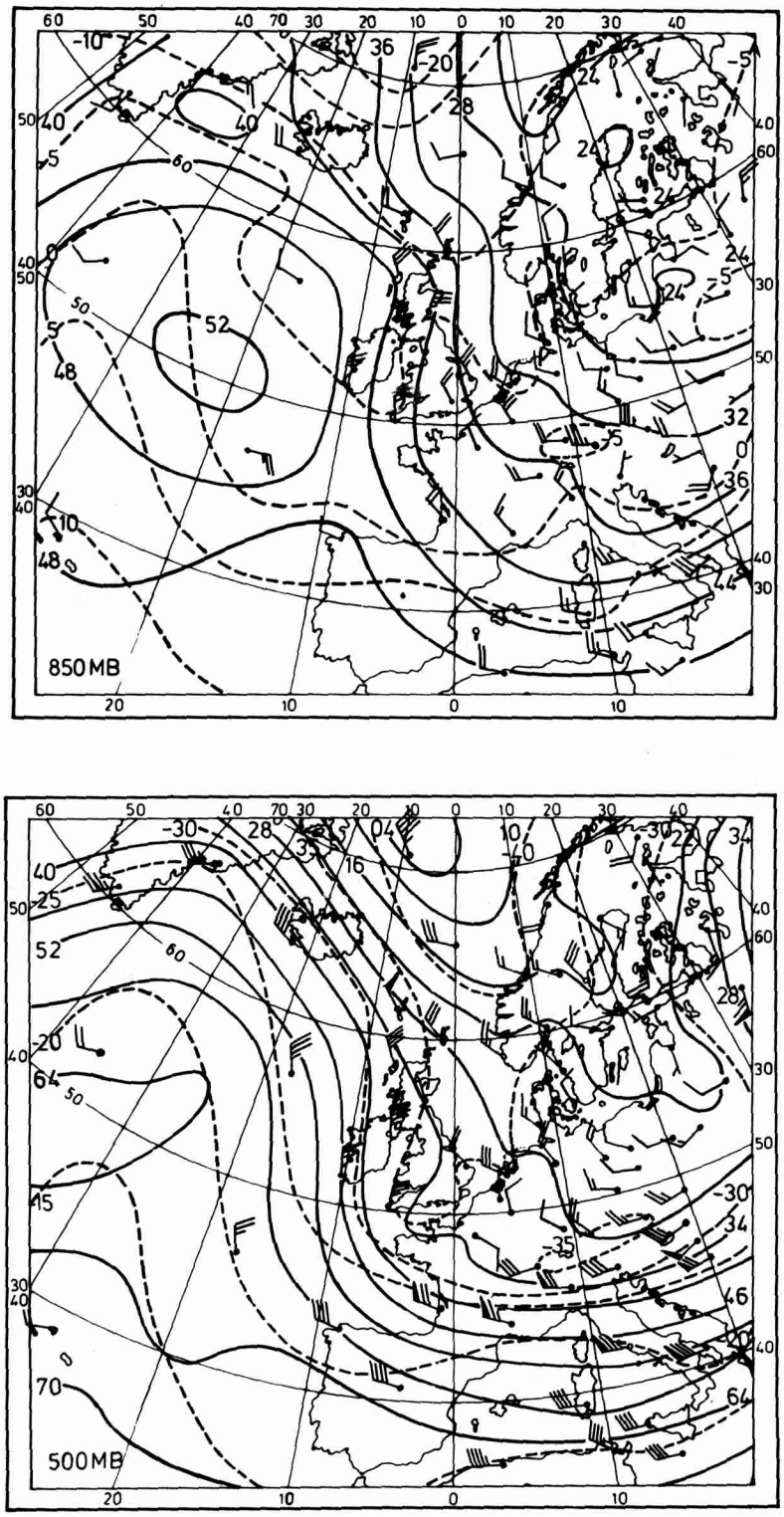

Figure 3. Analyses of the 850 and 500 mb levels of 00 GMT, 18 November 1977. The spacing of the isotherms (dashed lines) is 5°C. Isohypses are drawn at intervals of 40 and 60 gpm, respectively.

3. Pressure analysis

The first question arising is whether we can find a connection between the pattern of precipitation cells and the surface-pressure field. Hourly surface analyses did not show such a connection. However, the procedure outlined hereafter unmistakably brought to light that a well-defined eddy-pressure field existed.

Figure 4 shows the weather stations used in the analysis, which has been carried out as

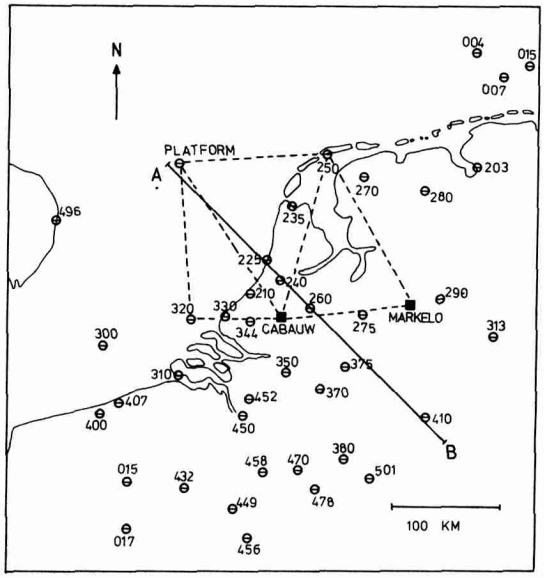

Figure 4. Weather stations used in the analysis. Black squares show the position of the research tower (Cabauw) and the television tower (Markelo) at which wind is measured. The dashed lines mark the triangles for which convergence and vorticity were computed. See also Fig. 6.

follows. At each station a series of hourly pressure readings running from 2100 to 0900 GMT was considered. In order to isolate the eddy pressure field, to each series a linear regression was computed and subtracted from the initial readings. The resulting series indicates the evolution of the eddy pressure field. It should be stressed that this procedure not only removes the linear pressure tendency but also systematic errors, such errors may be as large as 1 mb and completely mask features like the present one.

Figure 5 shows some results of the analysis. The eddy pressure curves all show the same shape. In November the daily cycle along the Dutch coast has a similar shape to these curves but has smaller magnitude; the dashed line shows this variation at the station where it is largest. The three maps in Fig. 5 present analysed eddy pressure fields during the most intense stage of the disturbance. If we compare these fields with the corresponding precipitation patterns (Fig. 1), we discover a striking correspondence between the location of the minimum of eddy pressure and the apparent centre of the disturbance. Clearly, at 03 GMT the eddy had a well-defined centre just off the Dutch coast. This centre split into two, but at 05 GMT only one centre was again present; at this time the eddy pressure reached its minimum value, about $-1{\cdot}2$ mb.

Although the disturbance was strong with regard to amount of precipitation, its pressure field is no more than a ripple of 1 mb. One may even argue that such a small pressure anomaly falls within the range of uncertainty associated with routine observations;

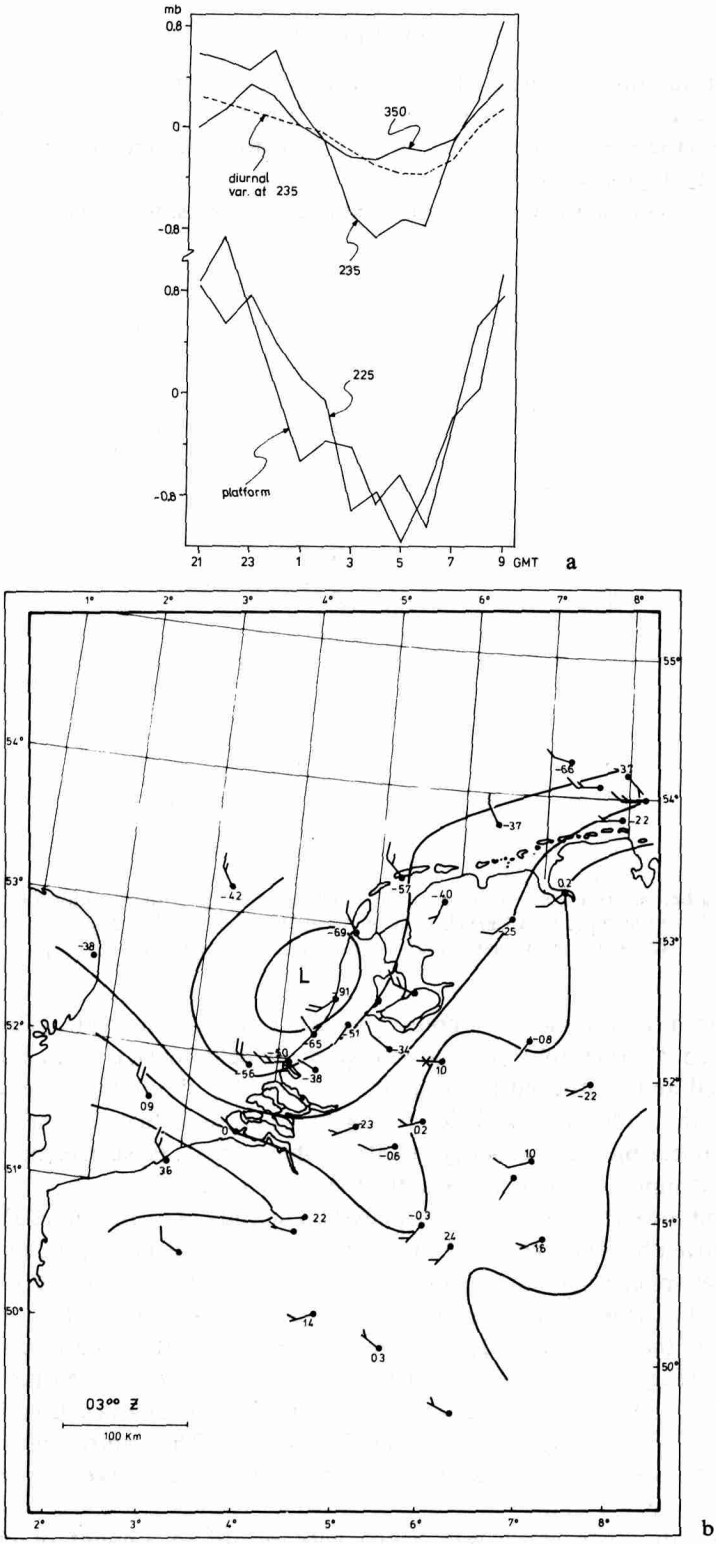

Figure 5. Eddy pressure analysis. The picture (a) (top) shows the eddy pressure as a function of time for a few stations. b, c and d are analyses of the eddy-pressure field during the period of maximum intensity. Spacing of the isobars is 0·25 mb.

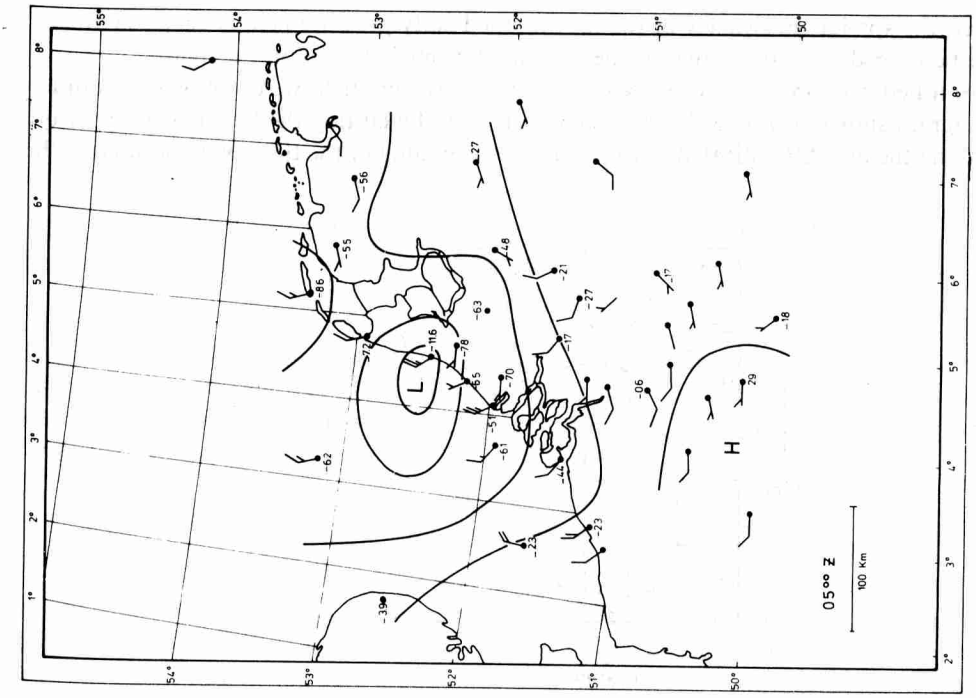

d

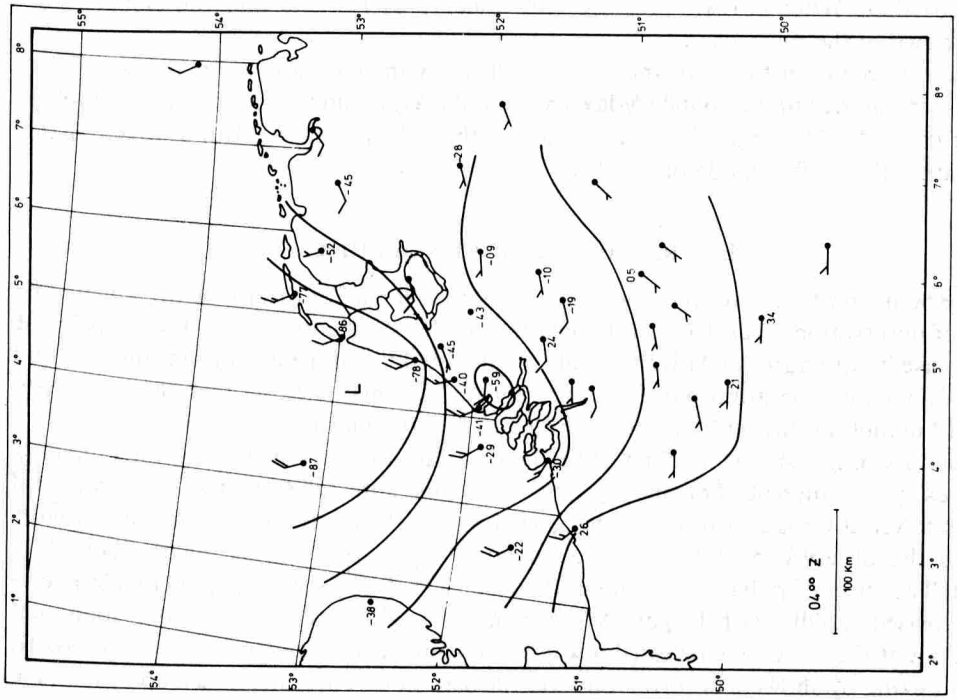

c

Figure 5. c and d.

however, the spatial consistency of the unsmoothed eddy pressure field is very convincing, as may be judged from the values at the various stations indicated in the figure.

For a better impression of the evolution of the pressure field we examine the running-time diagram shown in Fig. 6. It has been constructed by cutting the hourly eddy pressure fields along the line AB indicated in Fig. 4. In the beginning of the timespan considered, the

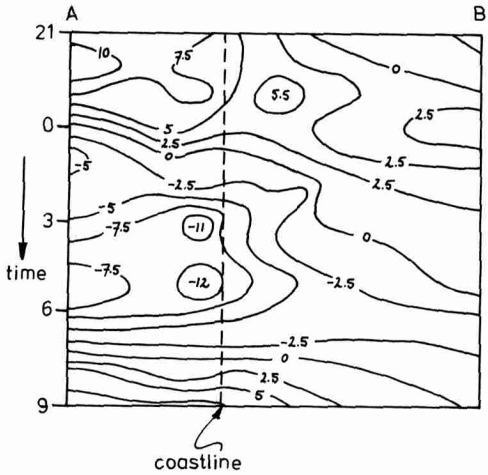

Figure 6. Running-time diagram of the eddy-pressure field along the line AB shown in Fig. 4. Unit is 0·1 mb.

isobars slope downwards to the right, indicating some advection of the eddy pressure field to the southeast. A weak ridge, which apparently caused the decrease of cloud amount during the evening, is clearly seen. At 01 GMT a weak trough (−0·5 mb) enters the region from the North Sea. Within two hours it develops to a separate centre that seems to linger at the coastline. After 06 GMT, pressure rises quickly everywhere and the isobars start sloping down to the right again.

Since the centre of the eddy appears to be fixed by the coastline, we may suspect that the land–sea contrast in the boundary-layer structure plays an important role in the development of the eddy. The pressure analysis suggests that we are dealing with a forced disturbance rather than a free mode of the flow.

4. The boundary-layer structure

The boundary layer over the southern part of the North Sea cannot be investigated by means of observations, but it is well known that under such unstable conditions as in the present case its structure is relatively simple. Undoubtedly, a large flux of sensible heat and water vapour into the atmosphere was present and we may assume that the windspeed increased monotonically with height according to the log.-linear wind profile.

Due to strong radiative cooling of the land surface during the evening, the boundary layer was quite different. Fortunately, measurements were taken at the meteorological research tower at Cabauw (for its location, see Fig. 4), which has a height of 200 m. Figure 7 shows the observed evolution of the boundary-layer structure during the period of interest. The effect of radiative cooling at the surface is clearly seen: the potential temperature increased rapidly with height. A sharp inversion did not appear; sodar soundings carried out at the same time revealed a weak inversion between 100 and 200 m. At 03 GMT, vertical mixing by showers occurred but after 06 GMT cloud cover decreased and the boun-

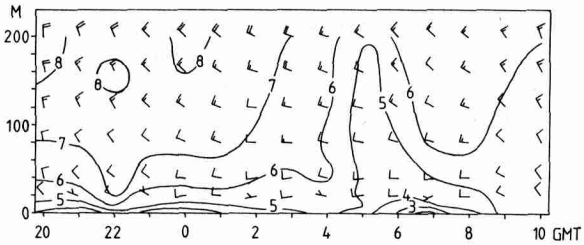

Figure 7. Wind and potential temperature as a function of height and time, measured at the Cabauw tower.

dary layer became stable again until sunrise. Wind veered with height throughout the period – note that this veering was less during the hours with shower activity. In fact, the features shown in Fig. 7 are in complete agreement with what we expect from theory and observational experience.

5. Divergence and vorticity

Knowledge of the magnitude of the vorticity and divergence above the boundary layer would aid the understanding of the nature of the disturbance. For this purpose, free atmosphere winds are needed. Since, over land, a stable layer was present, wind measurements taken at the surface do not give useful information. However, winds measured at the top of the Cabauw tower (200 m) and the television tower at Markelo (about 170 m, see Fig. 4) are probably close to the free atmosphere winds we need. Over the sea and along the coast the boundary layer was unstable, so it is possible to estimate the free atmosphere wind from the wind measured at a height of 10 m. This estimate was carried out by assuming that the free wind equals 1·6 times the 10 m. wind and that its direction is veered by 15°. Slightly different values of these constants were used to determine if such an arbitrary choice has a strong influence on the final results. The influence appeared to be restricted to the time-mean values of the divergence and vorticity. This is not a serious drawback because the main interest concerns the rate of change of these quantities.

With free winds obtained in this way, divergence was computed for the triangles indicated in Fig. 4. All triangles gave similar results: convergence in the evening and night, and divergence in the morning. Differences between the triangles were too small to escape the noise level (roughly given by the hour-to-hour variation). Vorticity was also computed. Again, all triangles showed a similar evolution: almost zero vorticity in the evening, gradually increasing during the night and decreasing again in the morning. Figure 8 presents the arithmetic mean values over the three triangles. Convergence and vorticity appeared to have the same order of magnitude, i.e. about $4 \times 10^{-5}\,s^{-1}$.

In order to relate those computations to the pressure analysis discussed in section 3, we have to take a look at the eddy vorticity and eddy convergence defined in the same way as the eddy pressure. So we consider the vorticity and convergence with respect to linear trends in these quantities. In Fig. 8 the trends are displayed by the dashed lines. They clearly indicate increasing vorticity, thus reflecting the weak trough that entered the region of concern.

During the first stage of the disturbance, the eddy vorticity is almost zero whereas the eddy convergence is positive. This convergence should create positive eddy vorticity through the action of the Coriolis acceleration, and indeed it seems to do so. Moreover, at the time the eddy convergence becomes negative (07 GMT) the eddy vorticity immediately starts to decrease. Since this picture is very realistic from a physical point of view, we conclude that

the computation of vorticity and convergence is valid and may be added to the diagnosis of the eddy. We finally note from Fig. 8 that both the vorticity and convergence were of order $10^{-5}\,s^{-1}$. The corresponding typical value of the eddy windspeed is roughly $1\,m\,s^{-1}$.

An attempt was made to compute a vertical profile of vorticity and convergence by using the rawinsonde ascents of Hemsby, Schleswig and St Hubert (at 00 GMT). Unfortunately, the results were extremely variable (with respect to height). A very weak indication

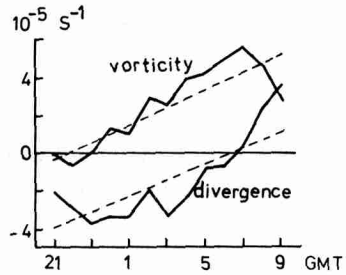

Figure 8. Vorticity and divergence in the lower troposphere computed from measured winds and averaged over the triangles shown in Fig. 4.

of low-level convergence and upper-level divergence showed up after removal of noise, but this result should be considered with caution.

6. Physical interpretation

In this section we will try to discover the basic mechanism that created the disturbance. Since the observational material is restricted, this necessarily involves speculation.

First, the correlation between the precipitation and eddy pressure fields suggests that the latent heat release played a major role in forcing the disturbance (the ability of latent heat release by convective activity to create small-scale cyclones has already been demonstrated by Nitta 1964). The latent heat release must have caused upward motion in the middle troposphere, thereby forcing upper-level divergence and low-level convergence. The convergence computations confirm this point.

An important feature of the present disturbance is the very rapid growth of the shower activity during the first hours of development (see Fig. 1). This points to the presence of potential instability which is suddenly released by the lifting of air in the lower part of the troposphere. The conditionally unstable air in the polar outbreak, in particular in the weak trough, was very suitable for such a process. Due to the high relative humidity in the lower layers, in principle only minor lifting was necessary to release the instability. This point is illustrated in Fig. 9. It shows profiles of equivalent potential temperature (θ_e) and equiva-

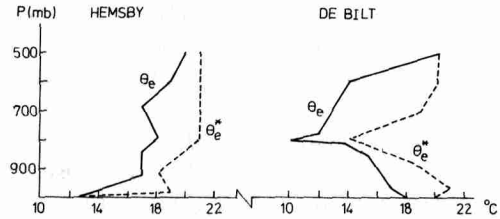

Figure 9. Equivalent potential temperature (θ_e) and saturated equivalent potential temperature (θ_e^*) at Hemsby and De Bilt, computed from the 00 GMT ascents.

lent potential temperature of a saturated atmosphere with the same temperature profile (θ_e^*), computed from the 00 GMT ascents of Hemsby and De Bilt. Since θ_e is a conservative quantity for pseudo-adiabatic processes, forced lifting is represented in the diagram by a straight line going upward. As soon as this line crosses the θ_e^* curve, spontaneous convection begins. From Fig. 9 we see that the air at De Bilt was potentially very unstable, while at Hemsby this was definitely not the case.

Once the convective precipitation occurs, the latent heat release creates additional lifting and low-level moisture convergence. It is not clear how crucial this moisture convergence is, because observed precipitation amounts only slightly exceeded the precipitable water content of the air mass.

Next, we have to determine the cause of the lifting. Since the region considered is very flat, orographic effects may be excluded. A frequently occurring mechanism creating low-level lifting is Ekman-layer pumping. For this to be effective, however, vorticity should be considerable. During the first stage of the disturbance, this was definitely not the case (see Fig. 8). Moreover, if normal Ekman-layer pumping did cause the lifting, it is not clear why the disturbance did not develop before the weak trough reached the coastal region. At this point we recall that during the night a stable layer developed over land whereas instability prevailed over sea. As may be seen in Fig. 5, the resulting frictional convergence along the coastline was pronounced. This may also be interpreted as a quasi-orographic effect: the stable layer over land appears as a hill (of stationary air) with a height of roughly 100 m. Figure 5 suggests that 20 km or so downstream of the coast the stable layer has developed, thus giving a slope of about 1/200. With a wind speed of $10\,\mathrm{m\,s^{-1}}$, this rough scaling yields a low-level vertical velocity of $5\,\mathrm{cm\,s^{-1}}$ in the coastal region. An analysis of Ekman-layer pumping (e.g. Holton 1972) shows that a relative vorticity of about $10^{-4}\,\mathrm{s^{-1}}$ would be needed to cause a comparable vertical velocity by this mechanism. We conclude that the crucial lifting was forced by differences in the boundary-layer structure over sea and land.

We now turn to the question why the disturbance disappeared so rapidly. Four effects should be mentioned, namely, (i) effect of latent heat release on the large-scale stability, (ii) breakdown of the stable layer over land due to vertical mixing forced by shower activity, (iii) lack of moisture supply from the surface over land, and (iv) no sensible heat supply over land. With regard to the small time-scale of the eddy, (i) and (iii) are probably less important. The lingering of the disturbance and its sudden breakdown indicate that (ii) and (iv) play an important role. Although the large sensible heat flux over sea is not required to initiate the convection (though, of course, contributing to the build-up of the potentially unstable air mass), it may be necessary at a later stage in which the air mass is less unstable. No matter which process is most important, the observational analysis strongly suggests that the sea–land contrast was crucial to the existence of the disturbance. Therefore it had to compete with advection by the mean flow. Apparently, the latent heat release kept pace with the advection for a couple of hours, thus maintaining the pressure perturbation. At a certain moment, however, the balance broke down, the eddy was advected to the southeast, and consequently the sensible and latent heat supply from the surface were cut off. This seems to be the most likely explanation for the decay of the eddy.

Summarizing, observations suggest that the eddy was a warm-core system driven by the release of latent heat and initiated by forced lifting at the coastline together with a weak passing trough. It should be regarded as an externally forced disturbance, and not as a free mode of the flow. The following scaling argument enforces this statement.

The horizontal length scale L of the eddy was about 150 km. With the appropriate characteristic wind speed V this provides an estimate of the time scale: $T = L/V$. If the eddy were a free mode, it would merely be advected by the mean flow (the β-effect may be neglected). Consequently, the appropriate value of V is the eddy wind speed itself, being

about $1\,\mathrm{m\,s^{-1}}$. In this way we obtain $T \simeq 40\,\mathrm{h}$. On the other hand, if the eddy is forced by differences in surface conditions, which do not move, advection by the mean flow strongly influences the evolution of the eddy, which means that the appropriate value of V should be the mean wind speed. Thus, with $V = 10\,\mathrm{m\,s^{-1}}$, we obtain $T \simeq 4\,\mathrm{h}$. The conclusion of this scaling is obvious: the second case applies to the disturbance we are studying.

Finally, we note that after 4 h the eddy wind field must still be far from geostrophic equilibrium. The fact that eddy divergence and eddy vorticity have the same order of magnitude confirms this point (Fig. 8). This explains the small eddy wind speed ($1\,\mathrm{m\,s^{-1}}$) and small pressure perturbation (1 mb).

7. Final remarks

The foregoing analysis has provided a plausible interpretation of the disturbance so clearly revealed by radar. Similar features occur frequently in the vicinity of the Dutch coast. They are well known to the Weather Service, but poorly studied and understood. In most cases more chaotic precipitation patterns occur; the present case must be considered a rather special one. In particular, the suddenly appearing organization and disorganization of rainbands (Fig. 1) is rarely seen.

Recently, the physics of subsynoptic and mesoscale disturbances occurring in middle latitudes have received more and more attention. Simple model studies have been carried out to investigate the potential importance of convection (e.g. Økland 1977; Rasmussen 1977) and baroclinicity in a shallow layer (Harrold and Browning 1969; Duncan 1978). In many cases these mechanisms probably work together. On the time-scale we are dealing with, modelling of the convective/mesoscale interaction becomes particularly difficult. The frequently employed assumption that the latent heat release equals the moisture convergence in the lower layers is now very doubtful, so a more explicit representation of the convective/mesoscale interaction is needed. Kreitzberg and Perkey (1976, 1977) developed a fairly detailed model with which this interaction is studied. Their results lend some support to the ideas used in this study.

In spite of the fact that only routine observations were available for this case study, they provided much information. The pressure data, in particular, showed a high degree of consistency for which the observers should be complimented. In the author's opinion, case studies such as this, though simple, may lead to a better understanding of the meso- and subsynoptic scale phenomena that so often change a day's weather completely.

Acknowledgments

I thank my collegues for the useful discussions we had during the course of this study. The effort of Mr G. W. Brouwer in gathering the main part of the data is highly appreciated.

References

Duncan, C. N. 1978 Baroclinic instability in a reversed shear flow, *Met. Mag.*, **107**, 17–23.

Harrold, T. W. and Browning, K. A. 1969 The polar low as a baroclinic disturbance, *Quart. J. R. Met. Soc.*, **95**, 710–723.

Holton, J. R. 1972 *An introduction to dynamic meteorology*, Academic Press, 319 pp.

Kreitzberg, C. W. and Perkey, D. J. 1976 Release of potential instability: Part I. A sequential plume model within a hydrostatic primitive equation model, *J. Atmos. Sci.*, **33**, 456–475.

1977 Release of potential instability: Part II. The mechanism of convective/mesoscale interaction, *Ibid.*, **34**, 1569–1595.

Nitta, T. 1964 On the development of the relatively small scale cyclone due to the release of latent heat by condensation, *J. Met. Soc. Japan*, **42**, 260–267.

Økland, H. 1977 On the intensification of small-scale cyclones formed in very cold air masses heated by the ocean, Institutt foı Geofysikk, Report No. 26, University of Oslo, 25 pp.

Rasmussen, E. 1979 The polar low as an extratropical CISK disturbance, *Quart. J. R. Met. Soc.*, **105**, 531–549.